

Hybrid scene Compression for Visual Localization

Federico Camposeco¹, Andrea Cohen¹, Marc Pollefeys^{1,2}, and Torsten Sattler¹

¹Department of Computer Science, ETH Zürich ²Microsoft

Abstract. Localizing an image w.r.t. a large scale 3D scene represents a core task for many computer vision applications. The increasing size of available 3D scenes makes visual localization prohibitively slow for real-time applications due to the large amount of data that the system needs to analyze and store. Therefore, compression becomes a necessary step in order to manage large scenes. In this work, we introduce a new hybrid compression algorithm that selects two subsets of points from the original 3D model: a small set of points with full appearance information, and an additional, larger set of points with compressed information. Our algorithm takes into account both spatial coverage as well as appearance uniqueness during compression. Quantization techniques are exploited during compression time, reducing run-time w.r.t. previous compression methods. A RANSAC variant tailored to our specific compression output is also introduced. Experiments on six large-scale datasets show that our method performs better than previous compression techniques in terms of memory, run-time and accuracy. Furthermore, the localization rates and accuracy obtained are comparable to state-of-the-art feature-based methods, while using a small fraction of the memory.

1 Introduction

Visual localization constitutes an essential step in 3D computer vision. It plays an important role in large scale Structure-from-Motion (SfM) [1–3] as well as in Simultaneous Localization and Mapping (SLAM) [4]. Visual localization is also a key task for both robotics and mobile device applications, such as self-driving cars [5], virtual reality, and augmented reality [6].

The most common approach to visual localization requires a sparse 3D scene, where each point is associated to a 3D position and one or more image descriptors [7, 8]. In order to localize a query image, a set of 2D-3D correspondences can be established by using descriptor matching between pixels in the image and 3D points in the scene. These matches can subsequently be used for robust pose estimation, which consists of RANSAC and a minimal pose solver [9].

Large scale structure-from-motion techniques [1, 3, 10–12] have allowed the computation of increasingly large 3D models which can reach a size of tens of millions of points. However, the memory, computation and bandwidth limitations of most embedded applications (such as robotics and mobile) impose a hard constraint on the scene size that can be handled in an acceptable time budget.

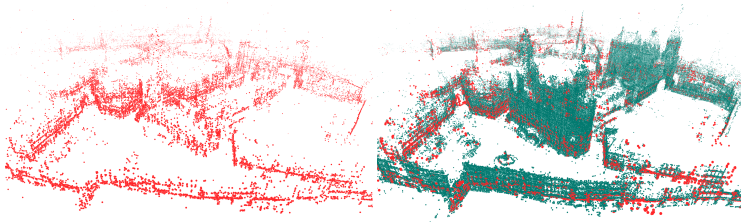


Fig. 1. Comparison of compressed scenes. On the left, the scene obtained using a state-of-the-art model compression scheme [13], and on the right, the output of our hybrid approach. Full-descriptor points are shown in red and compressed points in green. Both models use the same amount of memory, but ours leads to a better localization performance.

It is, thus, crucial to compress a 3D scene without (significant) loss in localization performance.

Previous works on 3D scene compression mostly fall under two categories: either the models are compressed by selecting a subset of all original 3D points and keeping their visual information (*i.e.*, full descriptors) [8, 13, 14], or all or a subset of the points are kept but their descriptors are compressed, *e.g.* [6, 15]. On a different line of work, CNN-based localization approaches such as PoseNet [16] implicitly represent a scene by the weights stored in a network, therefore also serving as a compression methods. However, CNN-based approaches have two main drawbacks: their localization performance is lower than feature-based methods [17] and they are also less flexible in the presence of scene changes.

In this paper, we present a hybrid 3D scene compression method that selects two subsets of scene points: the first subset consists of very few, carefully selected points with full descriptors, while the second, larger subset consists of points associated to quantized descriptors. The first set of points is used to obtain high-quality correspondences via full descriptor matching that can be used to generate pose hypotheses inside RANSAC. As the number of points in this set is very small due to memory requirements, they might not lead to enough matches for pose verification. Therefore, the second (and larger) set of points for which we only store compressed descriptors is used. While the resulting matches are not unique and thus cannot be used to generate pose hypotheses, they are sufficient for pose verification. Due to compressing the descriptors of the second set, our approach allows us to select significantly more points at the same memory consumption as standard approaches that store full descriptors per 3D point. One central insight of this paper is that having enough points for pose verification is important. As a result, our method performs better. We, therefore, show that storing these two sets of points provides more geometric information for localization while keeping the same memory consumption as other compression methods. An example of our compression output is visualized on the right in Fig. 1.

The first set of points is selected by taking into account three essential properties: *visibility*, *coverage* and *visual uniqueness* (also called distinctiveness). The

visibility of a 3D point is defined as the number of database images used from the 3D model that participated in the reconstruction of this point. A point with high visibility usually has a more accurate position, as well as a high probability of being seen by the device that needs to be localized. The second property, coverage, requires the compressed scene to cover the same area as the original scene. This increases the chance of localization anywhere in the original scene, even in less densely sampled areas. The uniqueness property is related to how visually distinctive a 3D point is w.r.t. all other points in the scene. Ideally, all 3D points in the compressed scene should be very different from each other in appearance, in order to filter out redundant information and reduce ambiguity during the localization process.

The second set of points is chosen in a simpler way, based only on visual uniqueness. Our algorithm scores the uniqueness of a 3D point by using descriptor quantization. Since this quantization step is useful for speeding up visual localization and for descriptor compression [6, 18], our method exploits this readily available information, thus adding uniqueness to the compression with almost no overhead.

This work also introduces a RANSAC variation for robust pose estimation that exploits the two types of 3D point subsets, as well as 3D point co-visibility by using a guided sampling strategy (inspired by [18, 19]) that aims to choose only co-visible 3D points to produce minimal subsets. This sampling strategy increases the chances of finding a good minimal sample, which can be critical for accuracy and performance when dealing with lower inlier ratios.

In short, this paper presents the following contributions:

- We propose a novel hybrid 3D scene compression algorithm that takes into account visibility, coverage and uniqueness. Both coverage and uniqueness are enforced using a novel technique that allows for better coverage while being faster than state-of-the-art.
- We obtain two different types of compressed points: spatially compressed but fully descriptive points that result in good unique matches, and a larger set of points compressed in appearance space that result in multi-matches. This second set of points has a low memory consumption while being very helpful for avoiding loss in localization performance.
- We introduce a novel RANSAC variant that uses a co-visibility-based sampling prior and exploits multi-matches for model evaluation during robust pose estimation. This modified RANSAC improves both successful localization rates and accuracy.
- We validate our method on six challenging large-scale datasets, showing that our compression scheme outperforms state-of-the-art methods both in terms of number of localized images, as well as pose estimation accuracy. [8, 16, 17, 20, 21].

2 Related Work

The literature on 3D scene compression for visual localization can be divided into three main categories: image retrieval techniques, neural network-based scene representations, and scene compression for feature-based localization methods.

Image retrieval techniques [15, 22, 23] perform compression by representing each image through a set of visual words (or using an even more compact representation such as the VLAD descriptor [24]), meaning that only little data needs to be kept in memory at all times. These methods may provide an approximate pose estimate via the known pose of the retrieved database images. In order to improve retrieval performance, [25] synthesizes a set of minimal views from the 3D scene in order to cover the whole scene and reduce memory requirements. As a next step, the data needed for accurate pose estimation can either be loaded from disk on demand (*e.g.* 3D points and their descriptors), or the local structure can be recomputed on the fly [26]. As such, the retrieval step is typically efficient, but the next stages are either slow due to loading from disk (which also does not solve the problem of compressing models such that they fit on robots or mobile devices) or due to heavy computations (solving a local structure-from-motion problem). Therefore, these methods trade in memory compression rate for run-time and are not fit for embedded applications.

Rather than matching local features, approaches such as PoseNet [16, 17, 20, 21] use CNNs for localization. Information about the 3D scene is stored implicitly in the network rather than explicitly in a point cloud. Since these networks typically have a small memory footprint, such approaches can also be considered as compression schemes. However, [17] shows that the pose accuracy of such networks is significantly worse compared to feature-based methods.

The approach presented in this paper falls under the third category: scene compression for localization methods based on 2D-to-3D descriptor matching. The main idea of these methods is to compress scenes by selecting a subset of points [8, 13, 14, 27] or by compressing the point descriptors [6, 15]. Our method introduces a hybrid of both techniques, showing that we can combine a set of points with full descriptors with a larger set of points with quantized descriptors. [6] presents an approach which combines both point selection with descriptor quantization. However, they use both compression techniques on top of each other, maintaining only one small set of points with quantized descriptors. The use of this double compression drastically reduces the localization rate. They compensate for this by combining localization with tracking of 3D points across multiple images. In contrast, we are interested in "lossless" compression, in the sense that we want to compress the scene with minimal loss in localization performance for a single given image.

[8] formulates scene compression as a K -covering problem: The new compressed scene is composed of a subset of points with high visibility such that at least K of them are seen from each of the database images used to construct the scene. As opposed to this method, our work modifies the K -covering formulation in order to enforce a more uniform distribution of the selected 3D points when projected into the database images. Instead of trying to cover K points per im-

age, we first divide each image into q uniform cells, and require the compressed scene to cover K/q 3D points per cell. This improves localization performance w.r.t. previous methods for the same compression rates.

Cao and Snavely [13] show that, although visibility is important when choosing the best subset of points to represent the 3D scene, the distinctiveness of the point descriptors should also be taken into account during compression. This ensures that points with an unique descriptor are selected, which improves matching performance, especially for high compression rates. Distinctiveness is introduced to the compression by checking that each new point added to the compressed scene has a minimum descriptor distance to all the points that have already been chosen. This procedure of comparing each new point to all previously selected points is computationally expensive, resulting in longer run-times for scene compression. In this work, we also extend the K -covering algorithm by taking distinctiveness into account. We show that it is sufficient to approximate similarity via quantization rather than explicitly computing descriptor distances. We exploit quantization both during K -cover to choose a proper set of distinctive and descriptive 3D points, as well as for selection and appearance compression of the second, larger subset of 3D points. The use of quantization allows us to decrease compression run-times considerably w.r.t. [13], while the use of our hybrid sets of points increases localization performance.

Similarly to our method, [15] also exploits one-to-many 2D-3D matches or multi-matches via quantization. However, they attempt to resolve these ambiguities before pose estimation by ensuring that matches are locally unique. Non-unique matches are simply discarded. In contrast, our work actively uses ambiguous multi-matches during the hypothesis evaluation step of pose estimation. This eliminates the chance of rejecting correct matches before RANSAC.

Scene points are said to be co-visible if they are seen together in at least one database image. Co-visibility has been explored, either for pre-RANSAC filtering [15, 18] or during RANSAC as a sampling strategy [19]. Pre-filtering based on co-visibility selects only matches that form a local cluster of co-visible points before pose estimation. Co-visibility-based sampling, on the other hand, is still subject to an initial random sample at each RANSAC iteration, therefore allowing RANSAC to explore different clusters of co-visible points and thus not suffering from early cluster elimination. Our sampling strategy is inspired by the co-occurrence-sampling introduced in [19].

3 3D Scene Compression

A 3D scene is composed of 3D points and database images. Each 3D point is associated to a set of SIFT descriptors corresponding to the image features from which the point was triangulated. These descriptors can then averaged into a single SIFT descriptor that describes the appearance of that point.

In order to localize a given image w.r.t. the 3D scene, 2D-to-3D matches are first established which are then used in RANSAC-based pose estimation [9]. As in [18], we employ a vocabulary-based approach to feature matching. Using

a pre-built vocabulary-tree, we first assign each 3D average descriptor to its corresponding K-means cell (visual word). At search time, each query image descriptor is assigned to its closest visual word w . We then select every 3D point in the scene that has the same visual word and search for a nearest neighbor in descriptor space among those selected points. As it will be seen next, we will make use of this vocabulary tree again at each step of the compression. This will allow us to both compress and query the 3D scene with a single visual vocabulary, which, as we will show, yields faster compression times and better localization performance w.r.t. previous compression methods.

After averaging the SIFT descriptors, most of the memory consumption of the 3D scene is concentrated in the averaged descriptors of the points. Therefore, we will aim to reduce memory consumption by 1) reducing the set of 3D points and 2) compressing the descriptor of a subset of non-Previously selected points using a visual word.

3.1 Reducing the Number of 3D Points

Let the initial set of 3D points be \mathcal{P} . The goal of compression is to select a subset $\mathcal{P}' \subset \mathcal{P}$ such that $|\mathcal{P}'|$ is minimal under the condition that \mathcal{P}' can be used to localize as many query images as possible. To tackle this problem, we begin with the assumption that the spatial distribution of query images will be close to the distribution of the database. This is an assumption also done in other works such as [8], and is in fact a sensible assumption to make.

We aim to select points such that each of the database cameras sees *enough* 3D points, *i.e.*, we want to enforce that each of the cameras in the database are *covered* by at least K points. As introduced by [8] the problem of choosing the optimal set of 3D points that cover all database cameras is an instance of the Set Cover Problem (or K -cover when at least K points must be seen from each camera). Furthermore, we recognize that by choosing two 3D points whose descriptors are too similar, a query image descriptor could be matched to either of those points resulting in ambiguities. This problem arises in the presence of repeated structures that produce very similar descriptors that are actually meters apart. Therefore, the *visual uniqueness* of the selected 3D points should also be taken into account.

Our primary concern is to select points which have a complete coverage of the scene, while penalizing points whose descriptors can be confused with other descriptors selected. We can thus, as proposed by [13], cast this problem into an instance of the Weighted K -cover problem [28], where K is the number of 3D points we require each image in the database to observe and the weight comes from the discriminative power of the descriptor associated with a point. Since the Weighted K -cover problem is NP-hard, we will employ a greedy approach in order to arrive at an approximate solution.

Let the binary matrix M represent the visibility graph (*i.e.*, the graph relating 3D points to cameras that see them) of the SfM model, where $M_{i,j}$ is 1 if the i -th image I_i observes the j -th point p_j . Starting from an empty set of selected

points \mathcal{P}' , our objective at each iteration is to find p_j that maximizes the gain

$$\mathcal{G}(p_j, \mathcal{P}') = \alpha(p_j, \mathcal{P}') \cdot \sum_{I_i \in \mathcal{I} \setminus C} M_{i,j} , \quad (1)$$

where C is the set of images that have already been covered by K points. For our particular problem, we would like the weights $\alpha(p_j, \mathcal{P}')$ to be computed according to a measure of how visually distinctive point p_j is w.r.t. the set of already selected points \mathcal{P}' .

In [13], α is computed by comparing the descriptor of each candidate p_j against all of the already selected 3D points. This produces a rather slow procedure, since each descriptor comparison can be costly and a search structure (such as KD-Tree) cannot be used due to the selected set changing at each iteration.

Instead, we exploit the fact that we perform vocabulary-based image localization using a pre-built vocabulary tree. As previously mentioned, we need to assign each 3D point to a visual word in advance to perform the 2D-to-3D matching. Thus, we may define the weighting term as

$$\alpha(p_j, \mathcal{P}') = 1 - \frac{|P'_w|}{\beta} , \quad (2)$$

where P'_w is the set of selected 3D points with descriptors assigned to the word w and β is the maximum number of allowed points per word (set to 10 in our experiments). We thus penalize the inclusion of 3D points whose visual word is too populated with a linear function. The intuition behind this being that the number of points assigned to a visual word gives an idea of how unique points in this visual word are.

As opposed to the work of [13], we opt to enforce that not only each image is covered by K 3D points but that the distribution of those points on the images is even. To do so, we subdivide the database images using a grid into q equal-area cells. We then regard the elements to be covered by the 3D points as image cells instead of images themselves. Let $c_h \in \mathcal{I}^c$, where $h = 1, \dots, q \times N$ and N is the total number of database images, be the h -th image cell to be covered. \mathcal{I}^c represents the set of all images cells and C^c the set of cells already covered. The final gain to maximize at each iteration is

$$\mathcal{G}(p_j, \mathcal{P}') = \alpha(p_j, \mathcal{P}') \cdot \sum_{c_h \in \mathcal{I}^c \setminus C^c} M_{i,j} . \quad (3)$$

Although the number of “cameras” to cover increases to $q \times K$, we found no noticeable increase in compression run-time since we also reduce the number of 3D points that are enforced to be viewed by each image cell to K/q . As we will show in Sec. 5, this has a positive impact on the localization rates, as the point selection has a more even coverage of the scene and prevents the selection process to be biased towards highly structured or textured parts of the scene, which might not necessarily be visible at query time. Additionally, a uniform distribution in 2D typically leads to more stable pose estimates compared to finding all matches in a single region of an image.

Once the greedy Weighted Set Cover algorithm is completed, we are left with a subset of 3D points $\mathcal{P}' \subset \mathcal{P}$ which should maximize scene coverage and descriptor uniqueness. Afterwards, the rest of the 3D points could be discarded (as in [13]). Instead, we choose to select a second subset $\mathcal{P}'' \subset \mathcal{P}$ of points for which only a compressed descriptor will be kept. This procedure is detailed next.

3.2 Selecting Multi-Matches

As previously mentioned, the most memory-consuming part of a 3D scene are the feature descriptors. As such, we may only select a small number of them to ensure that we substantially reduce the amount of memory required to represent a 3D model. If we only keep the matches selected using our Set Covering procedure, we are prone to miss matches due to the imperfect nature of the descriptors (features might not match due to large viewpoint changes) and the matching procedure. Additionally, only a few points might be visible in the query image as the database images are only an approximation to the set of all viewpoints. To mitigate this, we select a second subset of 3D points $\mathcal{P}'' \subset \mathcal{P} \setminus \mathcal{P}'$, where we will keep only the quantized descriptor (word assignment) for each selected 3D point and its 3D location. The purpose of this second subset of *compressed points* is the following: while the points in \mathcal{P}' result in high-quality matches that can be used for generating pose hypotheses during RANSAC, they might not be enough to properly verify these hypotheses. The set \mathcal{P}'' is thus used for verification. As these last matches are only used with a given hypothesis, they do not need to be unique as they are disambiguated by the pose. Therefore, they can be stored at little memory consumption.

We note that for each full 3D point we must store: a 3D coordinate, the full mean descriptor and a list of cameras that see the 3D point (which will be used within RANSAC to discard bad samples, see Sec. 4). For compressed points we only need to store: a 3D coordinate and one visual word index (1 integer). For 32-bit SIFT coordinates and a 32-bit visual word, we measure that in average we can store 26.5 compressed descriptor for each full descriptor. Since the only way of distinguishing compressed points is by their visual word, their selection process will thus focus on word uniqueness. To select the points for compression we use the following procedure: 1) score each point by their word occupancy (assigning a high score to low occupancy) and 2) select the X points that have the highest score. This procedure selects points without any regard to their camera coverage, however, this criteria has already been prioritized by the points selected in the first step of the compression.

Since we will, in general, have more than one 3D point with the same visual word, we must consider each 2D-to-3D match against compressed points as a *multi-match* (which will be handled differently within RANSAC in the next section). Nevertheless, the selection procedure for our compressed 3D points already minimizes the number of points in each word, therefore we can expect to have a low number of multi-matches per query descriptor.

4 Co-visibility-sampling and Multi-match RANSAC

As explained in Sec. 3, matching the 2D features of the query image against \mathcal{P}' using a standard ratio test as in [29] provides a set of one-to-one 2D-3D matches, which we will refer to as \mathcal{U} , while matching against \mathcal{P}'' results in a set of multi-matches or \mathcal{W} . The total set of matches will be referred to as $\mathcal{M} = \{\mathcal{U} \cup \mathcal{W}\}$. This section explains how \mathcal{M} can be used during the robust RANSAC-based pose estimation stage in order to improve both recall and run-time for localization when dealing with highly compressed scenes. The proposed algorithm is explained below and illustrated in Alg. 1.

Robust pose estimation is usually achieved by running RANSAC [9] with a minimal geometric pose solver (*e.g.* P3P [30] for the calibrated setting or P4P [31] for the unknown focal length case). A general RANSAC approach randomly selects minimal samples from \mathcal{M} , generates pose hypotheses with the minimal solver, and then evaluates these poses by counting the number of inliers according to a given threshold on the reprojection error. However, the lower the inlier ratio, the more samples are required by RANSAC to ensure that the correct pose is found with a certain probability. Indeed, the number of samples required increases exponentially with the outlier ratio. Therefore, our RANSAC variant limits the sampling only to the set \mathcal{U} of unique matches, since these matches have a higher probability of being actually good matches than those in \mathcal{W} . Indeed, using \mathcal{W} during the sampling stage potentially introduces a high number of outliers, resulting in a prohibitively large number of RANSAC iterations needed to find a good sample. Once a model has been sampled using only unique matches, it needs to be evaluated. Having a larger number of inliers increases the confidence in the quality of a sampled model. Therefore, the whole set of matches \mathcal{M} , including the multi-matches \mathcal{W} , is used to evaluate each pose.

In order to further reduce the number of RANSAC iterations, previous methods such as [32] use a guided-sampling strategy in order to increase the chances of finding a good sample. Inspired by this strategy, we propose a variation on the method introduced by [19] in the shape of a simple co-visibility-based sampling. Indeed, even in \mathcal{U} inlier ratios can be very small in a highly compressed scene, therefore, it is not enough to just limit sampling to this subset. It is desirable that samples should be drawn from sets of matches that correspond to co-visible points, *i.e.*, those that are seen from the same camera or neighboring cameras, as these matches have a higher chance of being geometrically consistent. Therefore, similarly to [19], our sampling should increase the probability of drawing from such subsets of matches.

More specifically, given $\mathcal{U} = \{m_j = s_j \leftrightarrow p_j\}$, where s_j denotes a 2D feature and p_j a 3D point, and n the cardinality of a minimal subset $\mathcal{S} \subset \mathcal{U}$, we would like all points $p_i \in \mathcal{S}$ to be co-visible. In [19], points are considered to be co-visible or co-occurring if they are all observed together in at least one database image. However, in practice, we found this definition of co-visibility to be a rather slow at sampling time due to the necessity of performing multiple set intersection.

We will therefore re-define co-visibility within a set of points $\mathcal{Q} = \{p_i, i = 1 \dots n\}$ given the set of database images in the 3D scene from which they were

reconstructed, referred to as $\mathcal{C}(p_i), p_i \in \mathcal{Q}$. The set \mathcal{Q} can be represented as a graph $\mathcal{G}_{\mathcal{Q}}$, where each point p_i is a node and an edge is added between a pair of points $p_i, p_j, i \neq j$ if they share at least one image in the scene, *i.e.*, $\mathcal{C}(p_i) \cap \mathcal{C}(p_j) \neq \emptyset$. We will consider \mathcal{Q} to be co-visible if each pair of points within \mathcal{Q} are at a maximum distance of 2 edges in the $\mathcal{G}_{\mathcal{Q}}$. We choose to enforce a simplified version of this constraint during sequential sampling of \mathcal{S} . As a first step, we randomly choose m_1 from \mathcal{U} to be the first element of \mathcal{S} . We sequentially draw the following m_i with $i = 2 \dots k$ samples and test whether they have an image in common with p_1 . If they do, then the sample m_i is accepted and included in \mathcal{S} . Otherwise, m_i is dropped and re-sampled while keeping in check a maximum number of failed sampling attempts F . Both for speed and simplicity, we choose to always look for intersections with $\mathcal{C}(p_1)$ instead of checking all of the points already in the subset as an approximation to our definition of co-visibility. To prevent the sampling of a minimal subset to get stuck when the initial choice of m_1 is not good enough, we put a limit on the number of sequential failed samples, and start over when this limit is reached. This simple sampling strategy ensures that only potentially good minimal subsets are chosen before doing pose estimation and evaluation.

Algorithm 1 Modified RANSAC

Require: Minimal subset size n , minimal solver PnP , matches $\mathcal{M} = \{\mathcal{U} \cup \mathcal{W}\}$, max. number F of sample trials, max. number T of iterations, inlier threshold σ

- 1: **repeat**
- 2: $\mathcal{S} = \emptyset, f = 0$
- 3: Randomly sample $m_1 = s_1 \leftrightarrow p_1$ from \mathcal{U}
- 4: $\mathcal{S} \leftarrow m_1$
- 5: **while** $|\mathcal{S}| < n$ **and** $f < F$ **do**
- 6: Randomly sample $m_i = s_i \leftrightarrow p_i$ from \mathcal{U}
- 7: **if** $\mathcal{C}(p_i) \cap \mathcal{C}(p_1) \neq \emptyset$ **then**
- 8: $\mathcal{S} \leftarrow m_i$
- 9: **else**
- 10: $f \leftarrow f + 1$
- 11: **if** $|\mathcal{S}| < n$ **then**
- 12: Jump to next iteration at line 1
- 13: Compute pose $\theta = PnP(\mathcal{S})$
- 14: **for all** $m_i \in \mathcal{M}$ **do**
- 15: **if** $e(m_i; \theta) < \sigma$ **then**
- 16: $Inliers(\theta) \leftarrow Inliers(\theta) + 1$
- 17: **if** $Inliers(\theta) > Inliers(\theta^*)$ **then**
- 18: $\theta^* \leftarrow \theta$
- 19: **until** T iterations are reached
- 20: **return** best model θ^*

5 Experimental Evaluation

In this paper, we focus on a hybrid scene compression that enables usage of a pre-computed 3D sparse scene for visual localization. Thus, for computationally constrained platforms we are specially interested in: 1. the run-time of the compression procedure, 2. the localization rate and memory reduction with respect to using an uncompressed scene and 3. the accuracy of the obtained poses.

In order to properly validate the proposed method, we evaluate it with 6 different real-world datasets (*cf.* Tab. 1). We chose these datasets since they are representative of the use-cases we aim to tackle with our method. By including datasets that have a wide variation in number of points and imaging conditions, we show that our methods can serve well in different scenarios. For the evaluation, we use SIFT [29] descriptors throughout and use a single 6K-word visual vocabulary, pre-computed using the Dubrovnik dataset. In practice, we did not observe strong evidence that suggested that using a vocabulary trained per dataset yielded consistently better results. This is also shown in [7]. For the pose computation, we use the P4P solver by [31].

This section is organized as follows: first, we do an ablation study that analyzes the impact of the compression method introduced in Sec. 3 and the RANSAC variant of Sec. 4. Next, the best setting of our method is compared against previous works, first in terms of compression run-time, registration (or localization) rates, and finally localization accuracy.

In Table 2 we compare four different settings of our method. We test its performance with and without image subdivisions and with and without our modified RANSAC. Notice that, when not using our modified RANSAC, we do not take into account \mathcal{P}'' and its corresponding multi-matches. As it can be seen from Table 2, there is a clear beneficial impact of each of the modifications proposed. Thus, in the following we will refer to using both image subdivisions and our modified RANSAC as “Our method”.

5.1 Compression Run-time

For each dataset in Table 1, we compress the scene to 1.5% of its size (factoring in both number of full-descriptor 3D points and multi-matches into this memory budget) and compare the run-times of our method to the state-of-the-art [13]. We have chosen 1.5% to be the default compression rate since it exhibits a good trade-off between performance and memory size. However, the relative speed-up in compression time of our method vs. [13] does not vary for different compression rates. Table 1 shows that we achieve consistently lower run-times than [13]. This is due to the fact that, as explained in Sec. 3, our method only needs to check the occupancy of a visual word to figure out the cost of selecting a 3D point.

5.2 Registration Rates

For the second experiment (see Fig. 2), we want to find the efficiency of our compression and pose estimation methods in terms of image registration power. Following [8, 13, 18, 19], we consider an image as registered if the best pose found by RANSAC has at least 12 inliers.

To make the compression rate comparison with [13] fair, we select a combination of compressed and non-compressed points in order to match the memory used by the selected 3D points in each experiment setting of [13]. This is done in the following way: for a given budget of M 3D points selected by [13], we divide the budget into two parts. The first 75% of the budget is utilized by selecting

Table 1. Datasets used and compression times (to 1.5%) for our method compared to “KCD” in [13] (using their implementation). The run-times for our method are significantly faster than those of [13]

Dataset	# DB images	# 3D points	# Query images	Compression Time [s]	
				Ours	KCD [13]
Dubrovnik [8]	6,044	1.88M	800	27.9	50.4
Aachen [33]	3,047	1.54M	369	21.6	45.5
King’s College [16]	1,220	503K	343	1.7	2.5
Old Hospital [16]	895	308K	182	3.6	12.5
Shop Facade [16]	231	82K	103	0.43	1.15
St Mary’s Church [16]	1,487	667K	530	8.74	26.1

0.75M uncompressed points by performing our weighted K -cover. The second 25% of the budget is then spent on compressed 3D points for multi-matches. The number of compressed points selected is actually larger than 0.25M, since we can store (on average) 26.5 compressed points for each full point (see Sec. 3). Thus, we select $0.25 \times 26.5M$ compressed points. For example, for a compression rate of 2.04% for Aachen, [13] selects 40,377 full 3D points while we select 30,282 full 3D points plus 267,517 compressed points for the same memory budget. We experimented with other rates of compressed vs full 3D points, and found that a 1:3 ratio was acceptable in all our 6 datasets. As can be seen from Fig. 2, our method vastly outperforms the state-of-the-art method by [13]. Notice, however, that all compared methods achieve consistently better performances for Dubrovnik vs Aachen. This might be due the different acquisition modes of these datasets. For Dubrovnik, the database images come from an internet photo-collection (Flickr) and thus tend to cluster around touristic areas. As such, good camera coverage can be achieved with fewer points. Since query images for this dataset were obtained randomly by removing images from a larger reconstruction of this dataset, they follow a similar distribution to the database images and can be correctly localized. For Aachen, the database images were taken more regularly to cover the area more completely, presenting less overlap between cameras. Thus, more points might be needed to properly cover all cameras. Additionally, query images were taken separately and do not follow the same distribution as the database images, therefore resulting in a harder to localize setting.

5.3 Localization Accuracy

Finally, we want to focus on the impact our scene compression method has on the accuracy of the resulting camera poses. To this end, we compare to state-of-the-art feature-based methods [8, 18, 34], as well as recent deep-learning-based methods [16, 17, 20, 21], as they also reduce the memory consumption of the localization database w.r.t. other feature-based methods. Results are shown for the Dubrovnik [12] dataset in Table 3 and the datasets from [16] in Table 4. The methods in [8, 18, 34] are similar to ours in that they also make use of

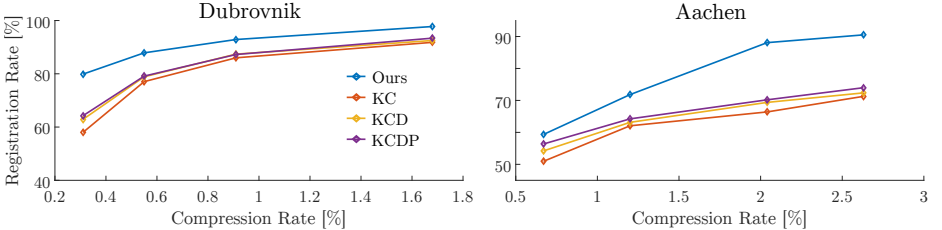


Fig. 2. Comparison of the registration rates (rate of the images localized) for different compression methods at different compression rates against the three methods in [13]. Notice that our method consistently outperforms the current state of the art for all compression rates.

Table 2. Comparison for all the variants of our method for the Dubrovnik dataset compressed to 1.5% of its original size. Where a • in “Grid” means we use image subdivisions and in MR stands for the usage of our modified RANSAC

Grid	MR	Median time (ms)		% reg. images	Median error	
		Query	RANSAC		Pos. (m)	Rot (°)
•	•	181	2.4	95.7%	2.09	0.42
		182	1.5	96.0%	2.02	0.37
	•	190	7.7	97.4%	2.09	0.39
		191	6.5	97.6%	1.97	0.35

SIFT features to localize a given query image to a sparse 3D scene. To compare the memory utilization of all methods, we make a coarse approximation of the memory used by simply multiplying the number of 3D points in a scene by the size in bytes that each descriptor occupies. We might in fact be underestimating the memory used in these non-compressed settings, as we are neglecting the storage occupied by the visibility information. For the deep learning methods, an approximate size of the network is shown.

It should be noted that the deep learning methods do not intrinsically provide a way to judge if a particular queried image was successfully localized (whereas in geometric methods one can rely on, *e.g.*, inlier statistics). Thus, registration rates cannot be fairly compared. As can be seen in Table 3 and Table 4, our method clearly presents the best trade-off between memory consumption and performance. It has been shown in [17] that the the feature-based Active Search method described in [18] performs better than any deep-learning methods, although this comes at a high-memory consumption cost. Thus, feature-based compressed methods represent the best of both worlds: they have a very small memory footprint (by up to orders of magnitude lower than non-compressed settings) while achieving a performance close to the state-of-the-art feature based methods.

Table 3. Accuracy for the Dubrovnik [12] dataset. Our method achieves a comparable accuracy and registration rate using only a few megabytes

Method	MB Used	#reg. images	Median pos. error
Ours (1.5% 3D pts)	3.79	782	1.87m
Active Search [18]	953	795	1.5m
P2F [8]	252.84	753	9.3m
PoseNet [20]	~50	-	7.9m
Voting [34]	252.84	798	1.69m

Table 4. Comparison with several state-of-the-art methods on the datasets from [16]

Method	King's College [16]			Old Hospital [16]			Shop Facade [16]			St Mary's Chruch [16]		
	MB used	# reg. images	Median errors [m, °]	MB used	# reg. images	Median errors [m, °]	MB used	# reg. images	Median errors [m, °]	MB used	# reg. images	Median errors [m, °]
Ours (@ 1.5%)	1.01	343	0.81, 0.59	0.62	178	0.75, 1.01	0.16	103	0.19, 0.535	1.34	530	0.50, 0.49
Active Search [18]	275	343	0.57, 0.7	140	180	0.52, 1.12	38.7	103	0.12, 0.41	359	530	0.22, 0.62
PoseNet [16]	50	-	1.92, 5.4	50	-	2.31, 5.38	50	-	1.46, 8.08	50	-	2.65, 8.48
Bayes PoseNet [21]	50	-	1.74, 4.06	50	-	2.57, 5.14	50	-	1.25, 7.54	50	-	2.11, 8.38
LSTMs [17]	~50	-	0.99, 3.65	~50	-	1.51, 4.29	~50	-	1.18, 7.44	~50	-	1.52, 6.68
σ^2 PoseNet [20]	~50	-	0.99, 1.06	~50	-	2.17, 2.94	~50	-	1.05, 3.97	~50	-	1.49, 3.43

6 Conclusion

In this paper, we have proposed a hybrid 3D scene compression scheme and a RANSAC variant that jointly manage to efficiently and accurately localize a given query image, all while using a small fraction ($\sim 1.5\%$) of the original memory usage. Differently to previously proposed methods, we compress the 3D scene by producing two disjoint sets of 3D points: 1. a set of points with their full visual descriptors that can be used to produce one-to-one matches given a query descriptor and 2. a second set of points for which we only store a compressed descriptor. This second type of points are used later to produce one-to-many matches, *i.e.*, multi-matches. The hybrid output of our compression scheme is carefully selected to ensure a good scene coverage and point visual uniqueness. To properly handle the special two-fold output of our compression, we design a RANSAC variant with two novel additions. First, we handle multi-matches such that they are only used during the model verification step, thus increasing number of inliers without negatively affecting the number of iterations. Second, we employ the co-visibility information (readily available in the 3D scene) directly within RANSAC to guide sampling.

We validate our approach using several real-world datasets and find that our method achieves state-of-the-art performance w.r.t. both feature-based and CNN-based methods, all while handling compression rates of less than 2% of the original scene.

Acknowledgements. We thank Google's Visual Positioning System for their support.

References

1. Schönberger, J.L., Frahm, J.M.: Structure-from-motion revisited. In: CVPR. (2016)
2. Agarwal, S., Snavely, N., Simon, I., Seitz, S., Szeliski, R.: Building rome in a day. In: ICCV. (2009)
3. Heinly, J., Schönberger, J.L., Dunn, E., Frahm, J.M.: Reconstructing the world* in six days*. In: CVPR. (2015)
4. Davison, A.J., Reid, I.D., Molton, N.D., Stasse, O.: Monoslam: Real-time single camera slam. PAMI **29** (2007) 2007
5. Häne, C., Heng, L., Lee, G.H., Fraundorfer, F., Furgale, P., Sattler, T., Pollefeys, M.: 3d visual perception for self-driving cars using a multi-camera system: Calibration, mapping, localization, and obstacle detection. IMAVIS **68** (2017) 14 – 27
6. Lynam, S., Sattler, T., Bosse, M., Hesch, J., Pollefeys, M., Siegwart, R.: Get out of my lab: Large-scale, real-time visual-inertial localization. In: RSS. (2015)
7. Sattler, T., Leibe, B., Kobbel, L.: Fast image-based localization using direct 2d-to-3d matching. In: ICCV. (2011)
8. Li, Y., Snavely, N., Huttenlocher, D.P.: Location recognition using prioritized feature matching. In: ECCV. (2010)
9. Fischler, M.A., Bolles, R.C.: Random sample consensus: A paradigm for model fitting with applications to image analysis and automated cartography. Communications of the ACM **24**(6) (1981)
10. Strecha, C., Pyvänäinen, T., Fua, P.: Dynamic and scalable large scale image reconstruction. (2010)
11. Frahm, J.M., Fite-Georgel, P., Gallup, D., Johnson, T., Raguram, R., Wu, C., Jen, Y.H., Dunn, E., Clipp, B., Lazebnik, S., et al.: Building rome on a cloudless day. In: ECCV. (2010)
12. Snavely, N., Seitz, S.M., Szeliski, R.: Modeling the world from internet photo collections. IJCV **80**(2) (2008) 189–210
13. Cao, S., Snavely, N.: Minimal scene descriptions from structure from motion models. In: CVPR. (2014)
14. Dymczyk, M., Lynam, S., Cieslewski, T., Bosse, M., Siegwart, R., Furgale, P.: The gist of maps - summarizing experience for lifelong localization. In: ICRA. (2015)
15. Sattler, T., Havlena, M., Radenovic, F., Schindler, K., Pollefeys, M.: Hyperpoints and fine vocabularies for large-scale location recognition. In: ICCV. (December 2015)
16. Kendall, A., Grimes, M., Cipolla, R.: Posenet: A convolutional network for real-time 6-dof camera relocalization. In: ICCV. (2015) 2938–2946
17. Walch, F., Hazirbas, C., Leal-Taixe, L., Sattler, T., Hilsenbeck, S., Cremers, D.: Image-based localization using lstms for structured feature correlation. In: ICCV. (2017)
18. Sattler, T., Leibe, B., Kobbel, L.: Efficient & effective prioritized matching for large-scale image-based localization. PAMI **39**(9) (2017) 1744–1756
19. Li, Y., Snavely, N., Huttenlocher, D., Fua, P.: Worldwide pose estimation using 3D point clouds. In: ECCV. (2012)
20. Kendall, A., Cipolla, R.: Geometric loss functions for camera pose regression with deep learning. In: CVPR. (2017)
21. Kendall, A., Cipolla, R.: Modelling uncertainty in deep learning for camera relocalization. In: ICRA. (2016)

22. Zhang, W., Kosecka, J.: Image based localization in urban environments. In: 3DPVT. (2006)
23. Philbin, J., Chum, O., Isard, M., Sivic, J., Zisserman, A.: Object retrieval with large vocabularies and fast spatial matching. In: CVPR. (2007)
24. Arandjelovic, R., Zisserman, A.: All about vlad. In: CVPR. (2013)
25. Irschara, A., Zach, C., michael Frahm, J., Bischof, H.: From structure-from-motion point clouds to fast location recognition. In: CVPR. (2009)
26. Sattler, T., Torii, A., Sivic, J., Pollefeys, M., Taira, H., Okutomi, M., Pajdla, T.: Are large-scale 3d models really necessary for accurate visual localization? In: CVPR. (2017)
27. Soo Park, H., Wang, Y., Nurnitadhi, E., Hoe, J.C., Sheikh, Y., Chen, M.: 3d point cloud reduction using mixed-integer quadratic programming. In: CVPR Workshops. (2013)
28. Lim, C.L., Moffat, A., Wirth, A.: Lazy and eager approaches for the set cover problem. In: Australasian Computer Science Conference. (2014)
29. Lowe, D.G.: Distinctive image features from scale-invariant keypoints. IJCV **60**(2) (2004) 91–110
30. Kneip, L., Scaramuzza, D., Siegwart, R.: A novel parametrization of the perspective-three-point problem for a direct computation of absolute camera position and orientation. In: CVPR. (2011)
31. Bujnak, M., Kukelova, Z., Pajdla, T.: A general solution to the P4P problem for camera with unknown focal length. In: CVPR. (2008)
32. Chum, O., Matas, J.: Matching with prosac-progressive sample consensus. In: CVPR. (2005)
33. Sattler, T., Weyand, T., Leibe, B., Kobbelt, L.: Image retrieval for image-based localization revisited. In: BMVC. (2012)
34. Zeisl, B., Sattler, T., Pollefeys, M.: Camera pose voting for large-scale image-based localization. In: ICCV. (2015)